THE JOURNAL OF BIOLOGICAL CHEMISTRY VOL. 287, NO. 41, pp. 34032–34043, October 5, 2012

ZIP8 Is an Iron and Zinc Transporter Whose Cell-surface Expression Is Up-regulated by Cellular Iron Loading*[S]

Received for publication, March 29, 2012, and in revised form, August 6, 2012 Published, JBC Papers in Press, August 16, 2012, DOI 10.1074/jbc.M112.367284

Chia-Yu Wang[‡], Supak Jenkitkasemwong[‡], Stephanie Duarte[‡], Brian K. Sparkman[§], Ali Shawki[§¶], Bryan Mackenzie[§], and Mitchell D. Knutson[‡1]

From the [‡]Food Science and Human Nutrition Department, University of Florida, Gainesville, Florida 32611, the [§]Department of Molecular & Cellular Physiology, and [¶]Systems Biology & Physiology Program, University of Cincinnati College of Medicine, Cincinnati, Ohio 45267

Background: Previous studies have identified the transmembrane protein ZIP8 (ZRT/IRT-like protein 8) as a zinc transporter.
Results: ZIP8 can transport iron in addition to zinc and is up-regulated by iron loading.
Conclusion: ZIP8 represents the third mammalian transmembrane iron import protein to be identified.
Significance: ZIP8 may play a role in iron metabolism.

ZIP8 (SLC39A8) belongs to the ZIP family of metal-ion transporters. Among the ZIP proteins, ZIP8 is most closely related to ZIP14, which can transport iron, zinc, manganese, and cadmium. Here we investigated the iron transport ability of ZIP8, its subcellular localization, pH dependence, and regulation by iron. Transfection of HEK 293T cells with ZIP8 cDNA enhanced the uptake of ^{59}Fe and ^{65}Zn by 200 and 40%, respectively, compared with controls. Excess iron inhibited the uptake of zinc and vice versa. In RNA-injected *Xenopus* oocytes, ZIP8-mediated $^{55}Fe^{2+}$ transport was saturable ($K_{0.5}$ of ~0.7 μM) and inhibited by zinc. ZIP8 also mediated the uptake of $^{109}Cd^{2+}$, $^{57}Co^{2+}$, $^{65}Zn^{2+} > {}^{54}Mn^{2+}$, but not ^{64}Cu (I or II). By using immunofluorescence analysis, we found that ZIP8 expressed in HEK 293T cells localized to the plasma membrane and partially in early endosomes. Iron loading increased total and cell-surface levels of ZIP8 in H4IIE rat hepatoma cells. We also determined by using site-directed mutagenesis that asparagine residues 40, 88, and 96 of rat ZIP8 are glycosylated and that *N*-glycosylation is not required for iron or zinc transport. Analysis of 20 different human tissues revealed abundant ZIP8 expression in lung and placenta and showed that its expression profile differs markedly from ZIP14, suggesting nonredundant functions. Suppression of endogenous ZIP8 expression in BeWo cells, a placental cell line, reduced iron uptake by ~40%, suggesting that ZIP8 participates in placental iron transport. Collectively, these data identify ZIP8 as an iron transport protein that may function in iron metabolism.

The mechanisms by which iron is taken up by mammalian cells are poorly understood except for those in just two cell types: the enterocyte and the erythroid precursor cell. Enterocytes take up dietary non-heme iron via transmembrane protein divalent metal-ion transporter-1 (DMT1)[2] located on the apical membrane (1, 2). In erythroid precursor cells, DMT1 transports iron from transferrin-containing endosomes to the cytosol (3). Accordingly, *Dmt1* (*Slc11a2*) knock-out mice display iron-deficient erythropoiesis and anemia, and intestine-specific *Dmt1* knock-out mice become progressively anemic after birth, likely because of an inability to absorb dietary iron (1). Interestingly, in *Dmt1* knock-out mice, most other tissues developed normally, including the liver, which displayed elevated concentrations of non-heme iron at postnatal day 3 (1). These observations demonstrate that alternative iron uptake pathways must exist. One such pathway may involve the plasma membrane protein ZIP14. Originally identified as a zinc transporter (4), ZIP14 was subsequently shown to transport iron in addition to zinc (5). In contrast to DMT1, which transports iron optimally at pH 5.2–5.5 (6–8), ZIP14 exhibits maximal iron transport at pH 7.5 (5, 9), making it well suited for iron uptake from the plasma, such as from non-transferrin-bound iron (NTBI) during iron overload. Endogenous ZIP14 in HepG2 hepatoma cells has additionally been detected in transferrin-containing endosomes, where it mediates, at least in part, the assimilation of iron from transferrin (10).

The ability of a ZIP family protein such as ZIP14 to transport iron is not without precedent. Indeed, the founding member of the ZIP family, IRT1 (iron-regulated transporter 1) in *Arabidopsis thaliana*, was identified as an iron transporter (11). As demonstrated by knock-out studies, IRT1 is responsible for iron uptake from the soil into the root (12). *Arabidopsis* IRT2, a close homolog of IRT1, was also found to be a high-affinity iron transporter (13). Additional ZIP family members that transport iron include ZupT in *Escherichia coli* (14) and LIT1 in *Leishmania amazonensis* (15).

* This work was supported, in whole or in part, by National Institutes of Health Grants R01 DK080706 (to M. D. K.) and R01 DK080047 (to B. M.) from NIDDK and Grant R24 CA086307 from the National Cancer Institute. This work was also supported by funds from the University of Cincinnati (to B. M.).
[S] This article contains supplemental Figs. S1–S5.
[1] To whom correspondence should be addressed: P.O. Box 110370, University of Florida, Gainesville, FL 32611. Tel.: 352-392-1991, ext. 204; Fax: 352-392-9467; E-mail: mknutson@ufl.edu.

[2] The abbreviations used are: DMT1, divalent metal-ion transporter-1; ZIP, ZRT/IRT-like protein; NTBI, non-transferrin-bound iron; EEA1, early endosome antigen 1; LAMP-1, lysosome-associated macrophage protein-1; TFR1, transferrin receptor 1; SFM, serum-free medium; NTA, nitrilotriacetic acid; ANOVA, analysis of variance.

Among the 14 mammalian ZIP family members, ZIP14 is most closely related to ZIP8 (16). Mouse ZIP14 and ZIP8 are similar in length (489 *versus* 462 amino acids), ~50% of their amino acids are identical, and they each contain a long extracellular N-terminal region with multiple potential glycosylation sites. Notably, ZIP14 and ZIP8 are 90% identical (19 of 21 amino acids) in putative membrane spanners IV and V, which have been proposed to form a metal translocation pore (17). Given the high degree of similarity between the two proteins, we considered the possibility that ZIP8, like ZIP14, would be able to transport iron. ZIP8 has been shown to transport zinc, cadmium, and manganese (18, 19), but measurement of iron uptake has not been reported. Therefore, the primary objective of the present study was to investigate the iron transport ability of ZIP8. We also assessed the regulation of ZIP8 by iron, its subcellular localization, and its expression levels in various human tissues. In addition, we determined which of the potential glycosylation sites of ZIP8 are glycosylated and whether glycosylation is required for metal transport.

EXPERIMENTAL PROCEDURES

Cell Culture—HEK 293T and H4IIE rat hepatoma cells were maintained in DMEM (Mediatech). BeWo cells were maintained in F-12K medium with L-glutamine (ATCC). All media were supplemented with 10% (v/v) FBS (Atlanta Biologicals), 100 units/ml penicillin, and 100 μg/ml streptomycin. The cells were maintained at 37 °C in 5% CO_2.

Expression of ZIP8 and Measurement of Iron and Zinc Uptake—HEK 293T cells were transiently transfected with rat ZIP8 (GenBank™ accession number BC089844) or empty vector pExpress-1 (Open Biosystems) for 48 h (FuGENE HD; Roche Applied Science). Prior to uptake, the cells were washed twice with serum-free medium (SFM) and incubated for 1 h in SFM containing 2% (w/v) BSA to deplete cells of transferrin and to block the nonspecific binding at 37 °C. For uptake, the cells were incubated with 2 μM [^{59}Fe]ferric citrate in SFM in the presence of 1 mM L-ascorbic acid for 2 h at 37 °C with or without a 10-fold molar excess of zinc, followed by three washes of iron chelator solution (1 mM bathophenanthroline sulfonate and 1 mM diethylenetriaminepentaacetic acid) to remove any surface-bound iron. The cells were lysed in buffer containing 0.2 N NaOH and 0.2% (w/v) SDS. Radioactivity was determined by γ counting, and protein concentration was determined colorimetrically by using the *RC DC* protein assay (Bio-Rad).

Expression of ZIP8 and ZIP14 in Xenopus Oocytes—We performed laparotomy and ovariectomy on adult female *Xenopus laevis* frogs (Nasco) under 3-aminoethylbenzoate methanesulfonate anesthesia (0.1% w/v in 1:1 water/ice, by immersion) following a protocol approved by the University of Cincinnati Institutional Animal Care and Use Committee. Ovarian tissue was isolated and treated with collagenase A (Roche Applied Science), and oocytes were isolated and stored at 17 °C in modified Barth's medium as described (20).

ZIP8 cDNAs for rat (GenBank™ accession number BC089844) and mouse (GenBank™ accession number BC006731) were subcloned into the pOX(+) oocyte expression vector between KpnI and NotI sites and under the SP6 promoter. ZIP8 cDNA-pOX constructs were linearized by using NotI and RNA was synthesized *in vitro* by using the mMESSAGE mMACHINE/SP6 RNA polymerase transcription kit (Applied Biosystems/Ambion) according to the manufacturer's protocol. We prepared mouse ZIP14 RNA from ZIP14-pOX(+) as described (2). Defolliculate stage V–VI oocytes were injected with 50 ng of RNA and incubated for 5 days (ZIP14) or 8–9 days (ZIP8) before being used in functional assays.

Functional Assays in Oocytes—We measured radiotracer metal-ion uptake in oocytes as described (2) or as follows. The oocytes were incubated at room temperature (23 °C) in transport medium containing 100 mM NaCl, 2 mM KCl, 2 mM $CaCl_2$, and 1 mM $MgCl_2$ and buffered using 0–5 mM 2-(*N*-morpholino)ethanesulfonic acid and 0–5 mM *N*′,*N*′-diethylpiperazine (GFS Chemicals, Columbus, OH) to obtain pH 7.5 or as otherwise indicated in Fig. 2*C*. Media containing Fe^{2+} or Cu^{1+} also contained 1 mM L-ascorbic acid; media containing Cu^{1+} or Cu^{2+} also contained 100 μM L-histidine. We used ^{55}Fe (added as $FeCl_3$) at a final specific activity of 220–340 MBq·mg^{-1}, ^{54}Mn (added as $MnCl_2$) at a final specific activity of 24 MBq·mg^{-1}, and ^{57}Co (added as $CoCl_2$) at a final specific activity of 0.4–2.9 GBq·mg^{-1}, each obtained from PerkinElmer Life Science Products (Boston, MA); ^{109}Cd (added as $CdCl_2$) at final specific activity 29 MBq·mg^{-1} and ^{65}Zn (added as $ZnCl_2$) at a final specific activity of 63 MBq·mg^{-1}, obtained from the National Laboratory (Oak Ridge, TN); and ^{64}Cu (added as $CuCl_2$) at a final specific activity of 2.0 GBq·mg^{-1}, obtained from Washington University-St. Louis (St. Louis, MO). Radiotracer metal-ion uptake was measured over 10 min, *i.e.*, well within the linear phase of uptake in oocytes expressing ZIP14 (2).

Concentration dependence data were fit by a modified Michaelis-Menten function (Equation 1) for which V^S is the velocity (uptake) of substrate S ($^{55}Fe^{2+}$ or $^{57}Co^{2+}$), V^S_{max} is the derived maximum velocity, S is the concentration of substrate S, and $K^S_{0.5}$ is the substrate concentration at which velocity was half-maximal.

$$V^S = \frac{V^S_{max} \cdot S}{K^S_{0.5} + S} \quad \text{(Eq. 1)}$$

Construction of HA-tagged ZIP8—A vector encoding rat ZIP8 with a C-terminal HA tag (YPYDVPDYA) was constructed by using inverse PCR mutagenesis (21). Briefly, full-length rZIP8 cDNA in pExpress-1 was used as the template with the following two 5′-phosphorylated oligonucleotide primers: 5′-GTGCCTGATTACGCCTAGCTGGGAGTATGACGTCAGCGCGG-3′ and 5′-GTCGTAAGGGTACTGCAATTCGATGTCCCCTGCGTACAAGG-3′ for the inverse PCR mutagenesis reaction. The PCR product was purified by using the QIAquick PCR purification kit (Qiagen) and subsequently digested with DpnI to eliminate template DNA. The digested PCR product was ligated by using T4 DNA ligase (New England Biolabs) and transformed into bacteria to obtain rZIP8-HA plasmid.

Subcellular Localization of ZIP8—HEK 293T cells were grown on poly-L-lysine-coated coverslips and transfected with rat ZIP8-HA. 48 h later, the cells were washed twice with PBS buffer containing 1 mM $MgCl_2$ and 0.1 mM $CaCl_2$ and fixed with

2% (w/v) paraformaldehyde for 15 min at room temperature. Excess paraformaldehyde was quenched by adding 50 mM NH_4Cl for 10 min, followed by three washes of PBS. To permeabilize cells, the cells were incubated with 0.1% (w/v) saponin for 10 min and then washed three times with PBS before blocking in 1% (w/v) BSA for 30 min. ZIP8-HA was detected by using mouse anti-HA primary antibody (1 μg/ml; Roche Applied Science) and rabbit anti-mouse IgG Alexa Fluor 594 secondary antibody (1:100; Invitrogen). To confirm permeabilization of cells, the lysosomal marker LAMP-1 (lysosome associated macrophage protein 1) was detected by using goat anti-LAMP-1 primary antibody (1:1000; Santa Cruz Biotechnology) and donkey anti-goat secondary antibody (1:100; Invitrogen). The endosomal marker, early endosome antigen 1 (EEA1) was detected by using goat anti-EEA1 primary antibody (1:1000; Santa Cruz Biotechnology) and the donkey anti-goat IgG Alexa Fluor 488 secondary antibody (1:100; Invitrogen). To stain nuclei, the cells were incubated with 10 μg/ml DAPI for 5 min and washed three times before mounting for confocal analysis using a Leica TCS SP2 laser scanning confocal microscope.

Generation of Rabbit anti-ZIP8 Antibody—Anti-ZIP8 antiserum was generated in rabbit against peptide (CDHTHFRNDDFGSKEK) that is conserved between mouse and rat ZIP8. Anti-ZIP8 antibodies were affinity-purified by using SulfoLink Coupling Resin (Thermo Scientific).

Iron Loading and Isolation of Cell-surface Proteins—To load cells with iron, H4IIE cells were treated with 100 or 250 μM ferric nitrilotriacetic acid (NTA) for 72 h. Cell-surface proteins were isolated by using the Pierce cell surface protein isolation kit (Thermo Scientific) according to the manufacturer's protocol. Briefly, H4IIE cells were incubated with EZ-Link Sulfo-NHS-SS-Biotin to biotinylate cell-surface proteins, which were subsequently affinity-purified by using NeutrAvidin-agarose resin (Thermo Scientific). Bound proteins were released by incubating with SDS-PAGE buffer containing 50 mM DTT.

Site-directed Mutagenesis of Potential N-linked Glycosylation Sites in Rat ZIP8—The QuikChange® Lightning site-directed mutagenesis kit (Stratagene) was used to mutate in rat ZIP8 asparagine residues at positions 40, 88, and 96 to aspartic acid or glutamine. The residues were mutated individually or in combination. All of the constructs were verified by DNA sequencing.

Assessment of N-linked Glycosylation—Cell lysates were digested with PNGase F to cleave *N*-linked glycans. Samples (30 μg protein) were denatured in buffer containing 1% (v/v) 2-mercaptoethanol and 0.5% (w/v) SDS at 37 °C for 30 min and then digested for 2 h at 37 °C with PNGase F (50,000 unit/ml of sample volume or 50 units/μg protein) (New England Biolabs). To inhibit *N*-glycosylation of endogenous ZIP8, H4IIE cells were incubated with tunicamycin (2 μg/ml) for 48 h.

Western Blot Analysis—Proteins were mixed with Laemmli buffer, incubated at 37 °C for 20 min, electrophoretically separated on a 7.5% polyacrylamide gel, and transferred to a nitrocellulose membrane (Schleicher and Schuell). The blot was blocked for 1 h in 5% (w/v) nonfat dry milk in Tris-buffered saline containing 0.1% (v/v) Tween 20 (TBST). The blots were then incubated overnight at 4 °C or 2 h at room temperature in blocking buffer containing 2.0 μg/ml mouse anti-HA (Roche Applied Science) or affinity-purified rabbit anti-ZIP8, mouse anti-transferrin receptor 1 (TFR1) (1:4000; Invitrogen), rabbit anti-scavenger receptor B1 (SR-B1) (1:2000; Novus Biologicals), mouse anti-tubulin (1:10,000; Sigma), or rabbit anti-CCS (1:5000; Santa Cruz Biotechnology). The membrane was washed four times for 5 min with TBST and incubated with the appropriate HRP-conjugated secondary antibodies. Immunoreactivity was visualized by using enhanced chemiluminescence (SuperSignal West Pico; Pierce) and x-ray film or the FluorChem E digital darkroom (Cell Biosciences).

Measurement of pH-dependent Iron Transport Activity in HEK 293T Cells—The pH-dependent iron transport activity was determined as previously described (20). Briefly, the uptake buffer (130 mM NaCl, 10 mM KCl, 1 mM $CaCl_2$, and 1 mM $MgSO_4$) was adjusted to pH 7.5, 6.5, and 5.5 by using HEPES or MES (2). HEK 293T cells transiently transfected for 48 h with mouse ZIP8 or empty vector (pCMV-Sport6) were washed twice with SFM and then incubated for 1 h in SFM containing 2% (w/v) BSA at 37 °C in 5% CO_2. For uptake, the cells were incubated with 2 μM [^{59}Fe]ferric citrate in uptake buffer in the presence of 1 mM L-ascorbic acid at 37 °C for 1 h.

Measurement of mRNA Levels—Total RNA from H4IIE cells was isolated by using RNABee (Tel-Test) according to the manufacturer's protocol. Relative mRNA levels of ZIP8, TFR1 1, and cyclophilin B in H4IIE cells were determined as described previously (22). Transcript copy numbers of ZIP8, ZIP14, DMT1, and TFR1 mRNA in human RNA (human total RNA Master Panel II; Clontech) were determined by using quantitative RT-PCR and standard curves generated from the plasmids pCMV-Sport6 human ZIP8 (BC012125; Open Biosystems), pCMV-XL4 human ZIP14 (BC015770; Open Biosystems), pBluescriptR−human DMT1 (BC100014, Open Biosystems), and pOTB7 human TFR1 (BC001188; ImaGenes). TaqMan primers and probes (Applied Biosystems) used for PCR were selected to target all known mRNA variants.

Suppression of ZIP8 Expression in BeWo Cells and Measurement of Iron Uptake—BeWo cells were reverse transfected with 50 nM siRNA targeting ZIP8 mRNA (FlexiTube siRNA; Qiagen) or AllStars Negative Control siRNA (Qiagen) by using Lipofectamine RNAiMAX (Invitrogen). After 72 h, cell lysates were prepared in radioimmune precipitation assay buffer and analyzed by Western blotting for ZIP8 as described above. For primary antibody, rabbit anti-human SLC39A8 (Prestige Antibodies; Sigma-Aldrich) was used at 1:5000 dilution. Iron uptake was performed as described for HEK293 T cells.

Statistical and Regression Analysis—Statistical and regression analyses were performed using SigmaPlot version 12 (Systat Software) with a critical significance level of $\alpha = 0.05$. Data for radiotracer uptake in oocytes were analyzed using two-way analysis of variance (ANOVA) followed by pairwise multiple comparisons using the Holm-Šidák test (adjusted P is reported). The data were fit by Equation 1 by using the least squares method of regression followed by F-tests of the significance of the fit to the model; S.E. is the standard error of the estimate, and P is the significance of the fit.

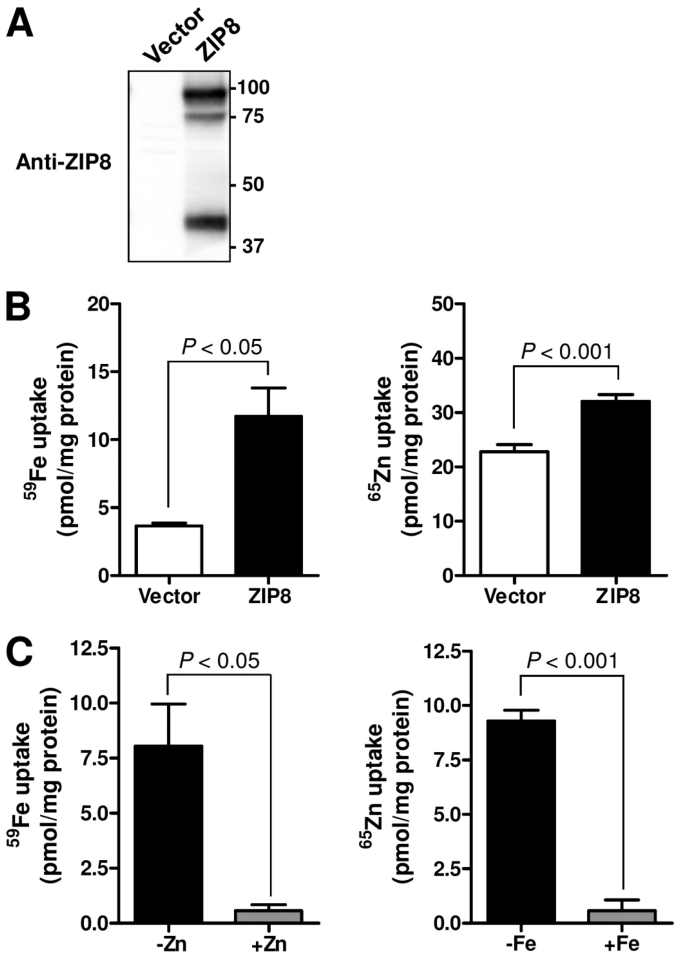

FIGURE 1. **Overexpression of ZIP8 increases the cellular uptake of iron and zinc.** *A*, Western blot analysis of ZIP8 in HEK 293T cells transiently transfected with empty pExpress vector or pExpress rat ZIP8. Total cell lysates were resolved by SDS-PAGE, transferred to nitrocellulose membrane, and immunoblotted with affinity-purified anti-ZIP8 antibody. *B*, cellular uptake of iron and zinc in HEK 293T cells overexpressing ZIP8. 48 h after transfection, the cells were incubated for 1 h in uptake medium containing 2 μM [^{59}Fe]ferric citrate or [^{65}Zn]$ZnCl_2$, and cellular uptake of ^{59}Fe (*left*) or ^{65}Zn (*right*) was measured by γ counting. *C*, mutual inhibition of iron and zinc uptake in cells overexpressing ZIP8. ^{59}Fe and ^{65}Zn uptake were measured in the presence of a 10-fold molar excess of unlabeled zinc (*left panel*) or iron (*right panel*). The amount of ^{59}Fe or ^{65}Zn taken up by cells is expressed as pmol/mg of protein. The data represent the means ± S.E. of three independent experiments. The treatment group means were compared by unpaired Student's *t* test.

RESULTS

Iron and Zinc Transport by ZIP8—Overexpression of ZIP8 in HEK 293T cells (Fig. 1*A*) was associated with a 200% increase in the uptake of ^{59}Fe compared with that in control cells transfected with empty vector (Fig. 1*B*). Consistent with the reported role of ZIP8 as a zinc transporter, cells transfected with ZIP8 cDNA displayed a 40% increase in the uptake of ^{65}Zn (Fig. 1*B*). The uptake of ^{59}Fe by ZIP8-expressing cells was inhibited >90% by a 10-fold molar excess of zinc (Fig. 1*C*). A 10-fold excess of iron likewise inhibited ^{65}Zn uptake. Uptake studies for iron were conducted in the presence of ascorbate so that uptake of Fe^{2+} could be directly assessed. Without ascorbate, iron uptake from ferric citrate requires a reduction step (likely via a cell-surface ferrireductase), which could affect uptake kinetics.

Metal-Ion Substrate Profile of ZIP8 Expressed in Xenopus Oocytes—Expression of rat ZIP8 strongly stimulated the uptake of 5 μM $^{109}Cd^{2+}$, $^{57}Co^{2+}$, $^{55}Fe^{2+}$, and $^{65}Zn^{2+}$ and, more weakly, the uptake of $^{54}Mn^{2+}$ in *Xenopus* oocytes at pH 7.5 (Fig. 2*A*). We found also that expression of mouse ZIP8 in oocytes similarly stimulated the uptake of 2 μM $^{55}Fe^{2+}$ ($p < 0.001$; data not shown). Expression of rat ZIP8 did not stimulate the transport of $^{64}Cu^{1+}$ or $^{64}Cu^{2+}$ (Fig. 2*A*). ZIP8-mediated $^{57}Co^{2+}$ transport (after subtraction of $^{57}Co^{2+}$ uptake in control oocytes) was saturable (supplemental Fig. S1) with half-maximal Co^{2+} concentration ($K_{0.5}^{Co}$) of ≈1.0 μM. We have previously demonstrated that mouse ZIP14, a close homolog of ZIP8, transports Cd^{2+}, Fe^{2+}, Mn^{2+}, and Zn^{2+} but not Cu^{1+} or Cu^{2+} (9), and found in the present study that mouse ZIP14 also transported Co^{2+} (supplemental Fig. S1). The substrate profile of ZIP8 therefore closely matches that of ZIP14.

Properties of ZIP8-mediated Iron Transport in Oocytes—ZIP8-mediated transport of $^{55}Fe^{2+}$ was strongly inhibited by 10-fold excess Co^{2+} and Zn^{2+} and more modestly by Mn^{2+} (Fig. 2*B*); this last observation is consistent with the much lower transport activity we had observed for $^{54}Mn^{2+}$ relative to Co^{2+} and Zn^{2+}. ZIP8-mediated transport of 2 μM $^{55}Fe^{2+}$ was markedly pH-dependent with optimal pH ≈7.5 (Fig. 2*C*). ZIP8 did not mediate significant $^{55}Fe^{2+}$ transport at pH 6.5 or below (Fig. 2*C*). Therefore ZIP8 is active over roughly the same pH range (for Fe^{2+} transport) as is ZIP14 (2). ZIP8-mediated $^{55}Fe^{2+}$ transport (after subtraction of $^{55}Fe^{2+}$ uptake in control oocytes) was saturable, and ZIP8 exhibited high affinity for Fe^{2+} (Fig. 2, *D* and *E*). The concentration at which Fe^{2+} transport was half-maximal ($K_{0.5}^{Fe}$) was ≈0.7 μM and did not significantly differ from $K_{0.5}^{Co}$) ($p = 0.27$, by Student's *t* test).

Subcellular Localization of ZIP8—For localization studies, we constructed an expression vector encoding rat ZIP8 with a C-terminal HA epitope tag. Western blot analysis of lysates from cells transfected with ZIP8 or ZIP8-HA cDNA revealed a similar band pattern when probed with anti-ZIP8 antibody (Fig. 3*A*). Two main immunoreactive bands were detected, one at ~100 kDa and the other at ~ 45 kDa. The latter band is similar to the 50.2-kDa theoretical molecular mass of rat ZIP8 (NCBI reference sequence NP_001011952.1), calculated from the amino acid sequence of the nascent peptide by using the ExPASy Compute pI/Mw tool. After the blot was stripped and reprobed with anti-HA antibody, the HA-tagged protein was detected, whereas the untagged protein was not (Fig. 3*A*). Detection of the same sized bands for ZIP8-HA with either the anti-ZIP8 antibody or anti-HA antibody confirms that the anti-ZIP8 antibody detects expressed rat ZIP8 protein.

To determine whether ZIP8 is expressed at the plasma membrane, HEK 293T cells were transfected with ZIP8-HA, fixed, and analyzed by immunofluorescence microscopy. The cells were analyzed without or with the detergent saponin to permeabilize the plasma membrane. In nonpermeabilized cells, strong plasma membrane staining was observed for ZIP8 (Fig. 3*B*), consistent with an exofacial C-terminal HA tag. Treatment with saponin permeabilized the cells, as indicated by the detection of the intracellular protein LAMP-1. In permeabilized cells, ZIP8 was detected not only at the plasma membrane but also widely throughout the cytosol in an apparent vesicular dis-

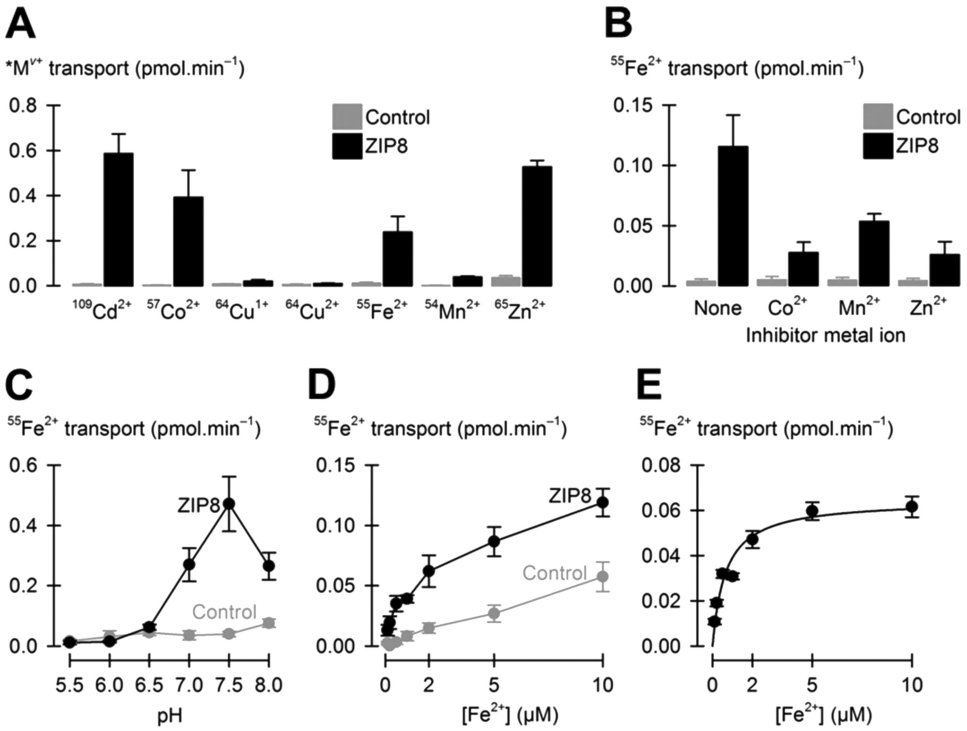

FIGURE 2. **Functional properties of ZIP8 expressed in *Xenopus* oocytes.** *A*, metal-ion substrate profile of rat ZIP8. Transport (uptake) of 5 μM metal ions ($^{*}M^{v+}$) was measured at pH 7.5 in control oocytes and oocytes expressing rat ZIP8. The data are the means ± S.D., $n = 14–19$ oocytes/group. Two-way ANOVA revealed an interaction ($p < 0.001$); Holm-Šidák pairwise comparisons within each metal revealed that uptake of Cd^{2+}, Co^{2+}, Fe^{2+}, Mn^{2+}, and Zn^{2+} differed between ZIP8 and control ($p < 0.001$ except for Mn^{2+}, $p = 0.016$), whereas uptake of Cu^{1+} ($p = 0.81$) and Cu^{2+} ($p = 0.47$) did not differ between ZIP8 and control. *B*, inhibition profile of ZIP8-mediated $^{55}Fe^{2+}$ transport. Transport of 1 μM $^{55}Fe^{2+}$ in control oocytes (*gray bars*) and in oocytes expressing ZIP8 (*black bars*) at pH 7.5 in the absence of inhibitor (*None*) or in the presence of 10 μM Co^{2+}, Mn^{2+}, or Zn^{2+}. The data are the means ± S.D., $n = 11–13$ oocytes/group. Two-way ANOVA revealed an interaction ($p < 0.001$); within ZIP8, all inhibitor metal ions differed from *None* ($p < 0.001$). *C*, transport of 2 μM $^{55}Fe^{2+}$ as a function of extracellular pH in control oocytes (*gray circles*) and oocytes expressing ZIP8 (*black circles*). The data are the means ± S.D., $n = 8–13$ oocytes/group. Two-way ANOVA revealed an interaction ($p < 0.001$); ZIP8 differed from control at pH 7.0 and higher ($p < 0.001$) but not at pH 6.5 and lower ($p \geq 0.22$); within ZIP8, transport differed for every pairwise comparison ($p < 0.008$) except between pH 7.0 and 8.0 ($p = 0.94$) and between pH 6.0 and 5.5 ($p = 0.87$). *D* and *E*, saturation kinetics of ZIP8-mediated $^{55}Fe^{2+}$ transport. Uptake of $^{55}Fe^{2+}$ was measured in control oocytes (*gray circles*) and oocytes expressing ZIP8 (*black circles*) at pH 7.5 (in *D*); the data are the means ± S.D., $n = 10–15$ oocytes/group. Mean uptake in control oocytes was subtracted from mean uptake in oocytes expressing ZIP8 to obtain mean ZIP8-mediated $^{55}Fe^{2+}$ transport (in *E*) ± propagated standard error. ZIP8-mediated $^{55}Fe^{2+}$ transport data were fit by Equation 1 (*solid black line*) yielding $V_{max}^{Fe} = 0.065 \pm 0.004$ pmol·min^{-1} and $K_{0.5}^{Fe} = 0.66 \pm 0.16$ μM (adjusted $r^2 = 0.94$; $p < 0.001$).

tribution. Colocalization studies (Fig. 3*C*) revealed that intracellular ZIP8 partially colocalized with EEA1, a marker of early endosomes. Because localization studies using overexpressed proteins can lead to artifacts, future studies will need to examine the localization of endogenous ZIP8.

pH-dependent Iron Transport Activity of ZIP8—The detection of ZIP8 in early endosomes of HEK 293T cells led us to consider a role for ZIP8 in iron transport from the acidic endosomal compartment. We therefore assessed the effect of pH on iron transport by ZIP8. Iron transport in HEK 293T cells was highest at pH 7.5 and then decreased with decreasing pH (Fig. 4). ZIP8-transfected cells displayed enhanced iron uptake at pH 6.5 but not at pH 5.5.

N-Glycosylation of ZIP8—Rat ZIP8 contains three potential *N*-linked glycosylation sites at residues 40, 88, and 96. We used site-directed mutagenesis along with Western blot analysis to investigate the glycosylation status of each of these sites. Mutation of each site independently (N40D, N88Q, or N96Q) increased the electrophoretic mobility of the expressed protein mutants compared with wild-type ZIP8 (Fig. 5*A*). The faster mobility of the mutant proteins is consistent with the prediction of fewer glycans. Accordingly, when two of the three sites were mutated in combination, the proteins migrated even faster, whereas the triple mutant protein (N40D/N88Q/N96Q) migrated the fastest. The immunoreactive band at ~100 kDa is approximately twice the size of the band at ~45 kDa, and both bands shifted down in parallel in the mutant proteins. These observations suggest that the ~100-kDa protein represents a dimer of the ~45-kDa protein. Iron transport studies with the triple mutant (N40D/N88Q/N96Q) protein revealed that *N*-linked glycans are not required for iron or zinc transport by ZIP8 (supplemental Fig. S4).

To determine whether endogenous rat ZIP8 is glycosylated, we used H4IIE cells, a rat hepatoma cell line. We chose to examine a liver-derived cell line because hepatocytes are able to take up NTBI as well as assimilate iron from transferrin (23, 24). The most prominent immunoreactive band in H4IIE lysates detected by anti-ZIP8 antibody migrated with an apparent molecular mass of ~140 kDa (Fig. 5*B*, *lanes 1* and *2*, and supplemental Fig. S2), similar to what others have shown in Western blot analyses of ZIP8 (25). ZIP8 was present at the cell surface because it could be isolated by using cell-surface biotinylation (Fig. 5*B*, *lanes 3* and *4*). Treatment of isolated cell-surface proteins with the endoglycosidase PNGase F shifted the cell-surface ZIP8 band from 140 to ~80 kDa, indicating that endogenous ZIP8 in rat H4IIE cells contains *N*-linked glycans.

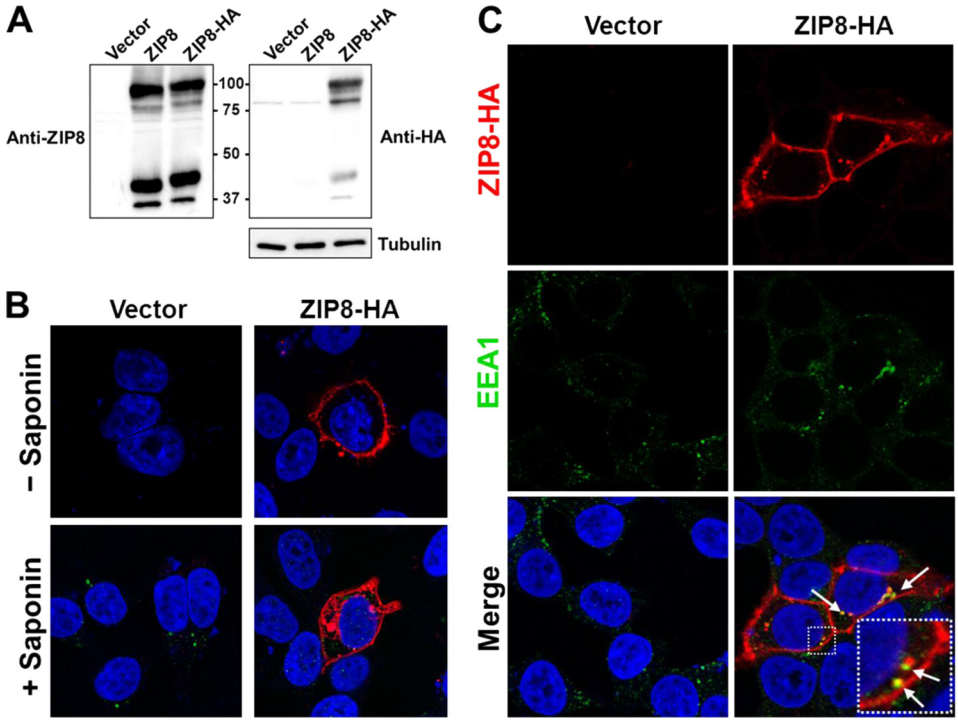

FIGURE 3. **ZIP8 expressed in HEK 293T cells localizes to the plasma membrane and intracellular vesicles.** *A*, Western blot analysis of ZIP8 and ZIP8-HA. HEK 293T cells were transiently transfected with empty pExpress vector, pExpress rat ZIP8, or pExpress rat ZIP8-HA. Total cell lysates were resolved by SDS-PAGE, transferred to nitrocellulose membrane, and immunoblotted with affinity-purified anti-ZIP8 antibody (*left panel*). The blot was then stripped and reprobed with an anti-HA antibody followed by an anti-tubulin antibody to indicate lane loading (*right panel*). *B*, detection of ZIP8 in nonpermeabilized and permeabilized cells. HEK 293T cells transiently transfected with pExpress empty vector or vector encoding ZIP8-HA were fixed and incubated without (−) or with (+) saponin to permeabilize cells. To detect ZIP8-HA, the cells were incubated with anti-HA primary antibody followed by Alexa Fluor 594-conjugated secondary antibody (*red*). As a control for permeabilization, all cells were coincubated with anti-LAMP1 primary antibody followed by Alexa Fluor 488-conjugated secondary antibody (*green*). The cells were analyzed by confocal fluorescence microscopy. *C*, colocalization of ZIP8 and EEA1. HEK 293T cells transiently transfected with pExpress empty vector or vector encoding ZIP8-HA were fixed, incubated with saponin, and analyzed for ZIP8 as described in *B*. To detect EEA1, the cells were coincubated with anti-EEA1 primary antibody followed by Alexa Fluor 488-conjugated secondary antibody (*green*). Merged images of ZIP8 and EEA1 reveal areas of colocalization (*yellow*), indicated by *arrows*. *Blue color* indicates nuclei counterstained with DAPI.

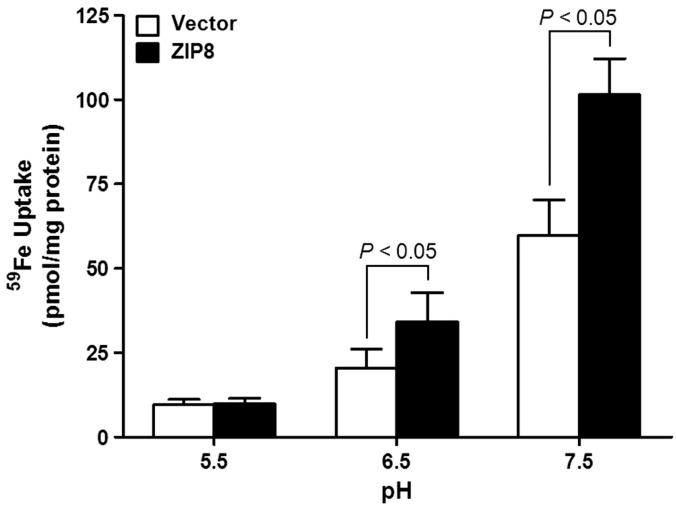

FIGURE 4. **pH dependence of ZIP8-mediated iron transport.** HEK 293T cells were transfected with empty pCMV-Sport6 vector or pCMV-Sport6 mouse ZIP8. 48 h after transfection, the cells were incubated with 2 μM [^{59}Fe]ferric citrate for 1 h in uptake buffer at pH 5.5, 6.5, and 7.5. The amount of ^{59}Fe taken up by cells is expressed as pmol/mg of protein. The data represent the means ± S.E. of three independent experiments.

Treatment of cells with the glycosylation inhibitor tunicamycin eliminated the immunoreactive ZIP8 band at 140 kDa and increased the intensity of the band at 100 kDa (Fig. 5*C*, *lanes 1* and *2 versus lanes 5* and *6*), suggesting that the 100-kDa band is a less glycosylated form of ZIP8. Additional treatment of lysates of tunicamycin-treated cells with PNGase F reduced the intensity of the 100-kDa band and increased the intensity of the 80-kDa band (Fig. 5*C*, *lanes 5* and *6 versus lanes 7* and *8*). Collectively, these observations suggest that the 100-kDa band is a partially glycosylated form of ZIP8, whereas the 80-kDa band is deglycosylated. The immunoreactive band detected at ~150 kDa in H4IIE cells appears to be nonspecific because it is unaffected by PNGase F (Fig. 5*C*, *lanes 1* and *2 versus lanes 3* and *4*) or tunicamycin (Fig. 5*C*, *lanes 3* and *4 versus lanes 7* and *8*).

Iron Loading and ZIP8 Expression—Treatment of H4IIE cells with either 100 or 250 μM iron-nitrilotriacetic acid (FeNTA) for 72 h increased ZIP8 levels 2- and 4-fold, respectively, as determined by Western blot analysis and densitometry (Fig. 6*A*). We used the level of TFR1, known to be decreased under high iron conditions (26), as an indicator of cellular iron loading in response to FeNTA treatment. Cell-surface biotinylation experiments revealed an increase in ZIP8 and a decrease in TFR1 abundance at the plasma membrane in cells treated with iron (Fig. 6*B*). The plasma membrane protein SR-B1 was measured to demonstrate enrichment of plasma membrane proteins isolated by cell-surface biotinylation, as well as equivalent lane loading. The cytosolic protein CCS (copper chaperone for superoxide dismutase) was detected in total cell lysate but not in isolated cell surface proteins, indicating that the isolated cell-surface extract was not contaminated with cytosolic proteins.

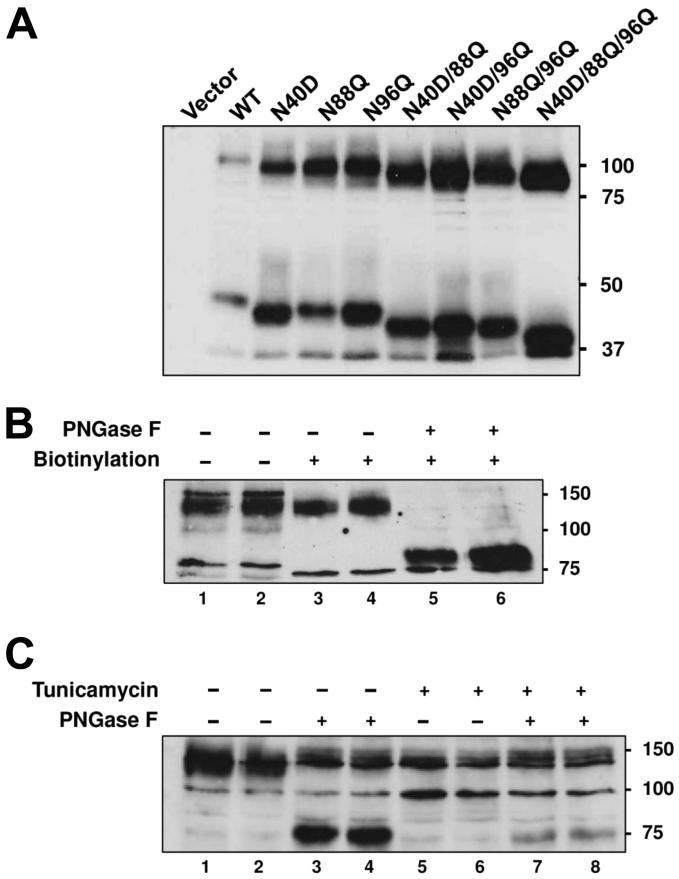

FIGURE 5. **Mutational analysis of potential *N*-linked glycosylation sites of rat ZIP8 expressed in HEK cells and glycosylation analysis of endogenous ZIP8 in H4IIE rat hepatoma cells.** *A*, Western blot analysis of WT rat ZIP8 and rat ZIP8 asparagine mutants expressed in HEK 293T cells. Asparagine residues 40, 88, and 96 of rat ZIP8 were mutated individually or in combination to aspartic acid or glutamine. *B*, Western blot analysis of cell-surface ZIP8 in H4IIE cell lysates treated without (−) or with (+) PNGase F. Cell-surface proteins were labeled with Sulfo-NHS-SS-Biotin and affinity-purified by using streptavidin-agarose prior to Western analysis. *C*, Western blot analysis of endogenous ZIP8 in H4IIE cells/cell lysates treated without (−) or with (+) tunicamycin or PNGase F. In *B* and *C*, *lane numbers* are indicated *below* the blots.

The higher ZIP8 levels in iron-loaded cells appear to result from post-transcriptional events because ZIP8 mRNA levels did not increase in response to iron loading (Fig. 6*C*), whereas TFR1 mRNA levels, used as a positive control for iron-related changes in gene expression, were substantially decreased in iron-loaded cells. Treatment of cells with zinc (40 μM zinc sulfate) increased ZIP8 levels, but the effect was transient, occurring at 3 h after treatment and not after 48 h (supplemental Fig. S3). The higher ZIP8 levels at 3 h were not associated with higher ZIP8 mRNA levels (data not shown), suggesting that zinc, like iron, regulates ZIP8 in a post-transcriptional manner.

Effect of FeNTA Treatment on Cellular Zinc Concentrations and Effect of Zinc Depletion on ZIP8 Levels—Although treatment of cells with FeNTA increases ZIP8 levels, it is possible that this effect is mediated through a secondary zinc deficiency induced by the high iron treatment. To examine this possibility, we treated cells with FeNTA and then measured total cellular iron and zinc concentrations by ICP-MS. As a positive control for zinc depletion, we included cells that were treated with the zinc-specific chelator, TPEN, which decreased zinc concentrations in H4IIE cells by 60% but did not affect iron concentrations (supplemental Fig. S5*A*). We found that treatment of cells with 250 μM FeNTA increased cellular iron levels 12-fold and decreased zinc concentrations by 30% (supplemental Fig. S5*A*). To determine whether zinc deficiency could independently increase ZIP8 levels, we measured ZIP8 levels in lysates from cells treated with TPEN. Western blot analysis revealed that zinc deficiency alone did not increase ZIP8 levels, whereas treatment with iron did (supplemental Fig. S5*B*). We therefore conclude that ZIP8 levels increase in iron-treated cells in response to iron loading but not zinc depletion.

Tissue Expression of ZIP8—To determine where ZIP8 is expressed, we measured mRNA copy number in RNA isolated from 20 different human tissues. Most abundant ZIP8 expression was detected in lung and placenta followed by salivary gland and thymus (Fig. 7). Tissues expressing the lowest amount of ZIP8 included skeletal muscle, fetal brain, testis, fetal liver, and small intestine. To compare the tissue distribution and expression levels of ZIP8 to other known proteins involved in cellular iron import, we measured mRNA copy numbers of ZIP14, DMT1, and TFR1. Similar to previous studies, ZIP14 mRNA levels were highest in liver and heart (4), DMT1 mRNA was abundantly expressed in kidney, brain, and thymus (2), and TFR1 was abundantly expressed in placenta (27).

Iron Transport Activity of Endogenous ZIP8—To examine iron transport activity of endogenous ZIP8, we measured iron uptake in BeWo cells in which ZIP8 was suppressed by using siRNA. BeWo cells, a placental cell line derived from a human choriocarcinoma, are widely used as a model to study placental uptake of nutrients including iron (28). In BeWo cells treated with ZIP8 siRNA, ZIP8 protein levels were reduced by 90% compared with control cells treated with negative control siRNA (Fig. 8*A*). After suppression of ZIP8, iron uptake was reduced by 37% (Fig. 8*B*), suggesting that ZIP8 mediates, at least in part, iron uptake by BeWo cells.

DISCUSSION

The present study establishes that ZIP8 can mediate the cellular uptake of iron, making it the third mammalian transmembrane iron import protein to be identified. ZIP8 was first identified in 2002 in a screen of monocyte cDNAs induced by infection and inflammatory stimuli (18). The amino acid sequence of ZIP8 was found to share significant homology to the zinc transporters ZIP1 and ZIP2, and therefore ZIP8 was postulated to function as a zinc transporter. Support for this possibility was provided by the observation that CHO cells stably transfected with ZIP8 accumulated and retained more zinc, as demonstrated by using an intracellular zinc-selective fluorescent dye (18). The first characterized mammalian iron importer, DMT1, was identified by screening an iron-deficient rat duodenal cDNA library for iron transport activity in *Xenopus* oocytes (2). The second protein found capable of transporting iron into mammalian cells was ZIP14, which had been originally described as a zinc transporter (29). Iron uptake via ZIP14 was demonstrated in HEK 293T and Sf9 insect cells that overexpressed the protein and then later in the *Xenopus* oocyte expression system (5, 9). Here we document the iron transport

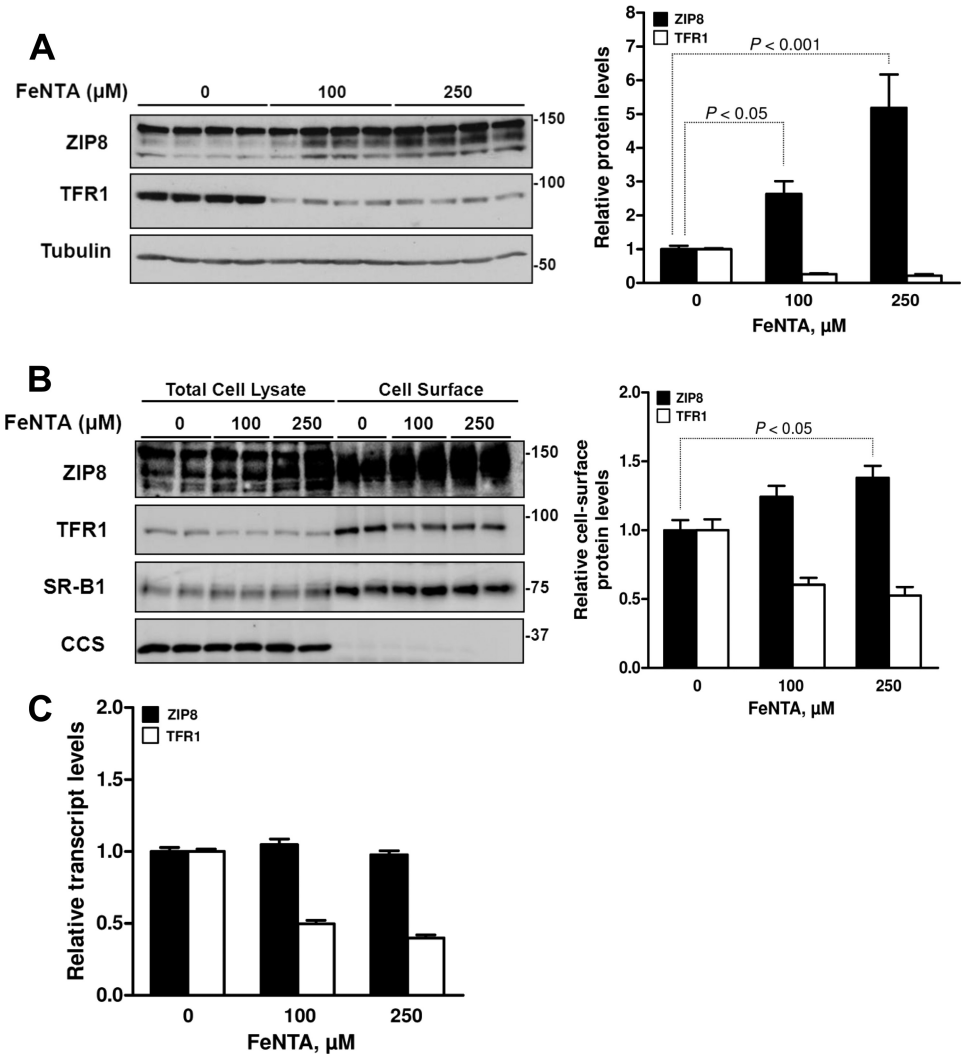

FIGURE 6. **Iron loading increases ZIP8 levels in H4IIE rat hepatoma cells.** *A*, Western blot analysis of ZIP8 in cells treated for 72 h with 0, 100, or 250 μM FeNTA. Total cell lysates were resolved by SDS-PAGE, transferred to nitrocellulose membrane, and immunoblotted with anti-ZIP8 antibody. The blot was then stripped and reprobed with an anti-TFR1 antibody followed by an anti-tubulin antibody to indicate lane loading. Relative protein levels of ZIP8 and TFR1, normalized to levels of tubulin, were determined by densitometry. *B*, Western blot analysis of ZIP8, TFR1, SR-B1, and CCS in total cell lysate and cell-surface proteins isolated from cells treated for 72 h with 0, 100, or 250 μM FeNTA. Cell-surface proteins were labeled with Sulfo-NHS-SS-Biotin and affinity-purified by using streptavidin-agarose prior to Western analysis. Relative cell-surface protein levels of ZIP8 and TFR1, normalized to levels of SR-B1, were determined by densitometry. *C*, relative mRNA levels of ZIP8 and TFR1 were determined by using quantitative RT-PCR. The data represent the means ± S.E. of three independent experiments. Treatment group means were compared by one-way ANOVA.

activity of ZIP8 by using both transfection of HEK 293T cells and expression in *Xenopus* oocytes.

Like ZIP14, we found that ZIP8 transports iron at physiologic pH, is expressed at the cell surface, and mediates the uptake of iron from ferric citrate, the predominant form of NTBI in the plasma of individuals with iron overload (30). Although these observations suggested a role for ZIP8 in NTBI uptake, we found that ZIP8 is not abundantly expressed (at least according to mRNA copy number) in liver, the primary organ that clears NTBI (31), or the heart, which also takes up NTBI (32). On the other hand, ZIP8 has been reported to be abundantly expressed in human pancreas (18), which was not represented in our RNA panel. After the liver, the pancreas is the organ that takes up the most NTBI (31). Our data in H4IIE hepatoma cells showing that iron loading increases plasma membrane levels of ZIP8 suggest that ZIP8 may be recruited to the cell surface to enhance the uptake of NTBI. Indeed a number of studies have shown that iron loading of hepatocytes increases the uptake of NTBI (33–36). Iron loading has also been shown to increase the uptake of NTBI by cardiomyocytes (33). Iron-mediated cardiotoxicity is the main cause of death in β-thalassemia major patients, who eventually succumb to iron overload because of repeated blood transfusions (37). Interestingly, microarray analysis found that ZIP8 mRNA levels were 1.8-fold higher in cardiomyocytes from β-thalassemic mice compared with wild-type controls (38). By contrast, DMT1 mRNA levels in cardiomyocytes from β-thalassemic mice were down-regulated 1.7-fold, whereas the levels of ZIP14 were apparently unaffected. Future studies should explore the contribution of ZIP8 to NTBI uptake in hepatocytes and cardiomyocytes, as well as other cell types susceptible to iron overload.

Treatment of H4IIE cells with zinc increased ZIP8 levels (although transiently), suggesting that ZIP8 actively participates in cellular zinc acquisition. As a zinc transporter, ZIP8 is

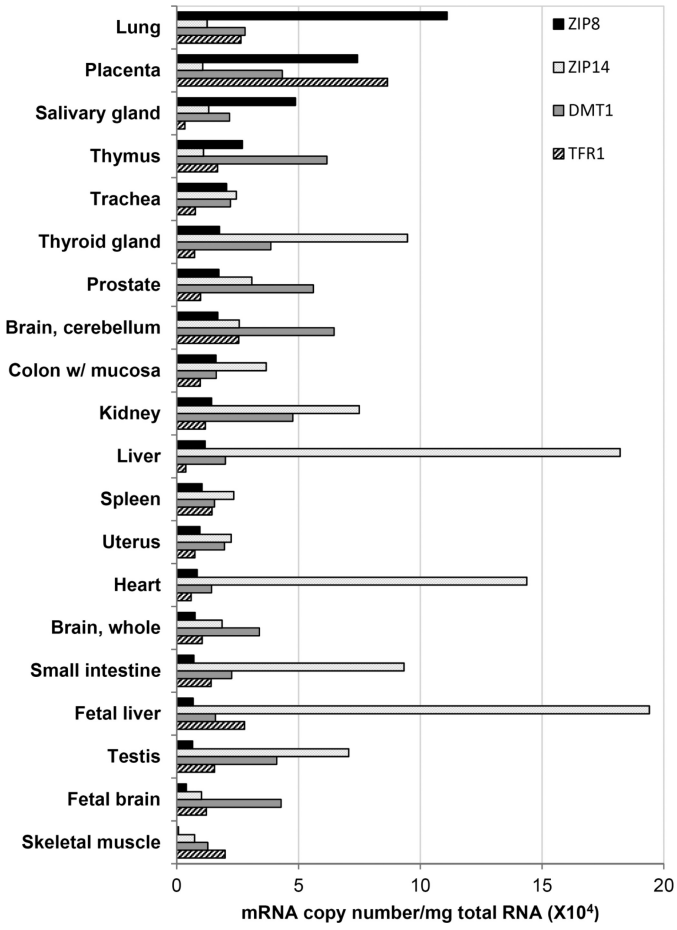

FIGURE 7. **Tissue expression of ZIP8, ZIP14, DMT1, and TFR1.** Tissue expression profiles were determined by using the human total RNA Master Panel II derived from 20 different tissues (Clontech). Transcript copy numbers were determined by using quantitative RT-PCR.

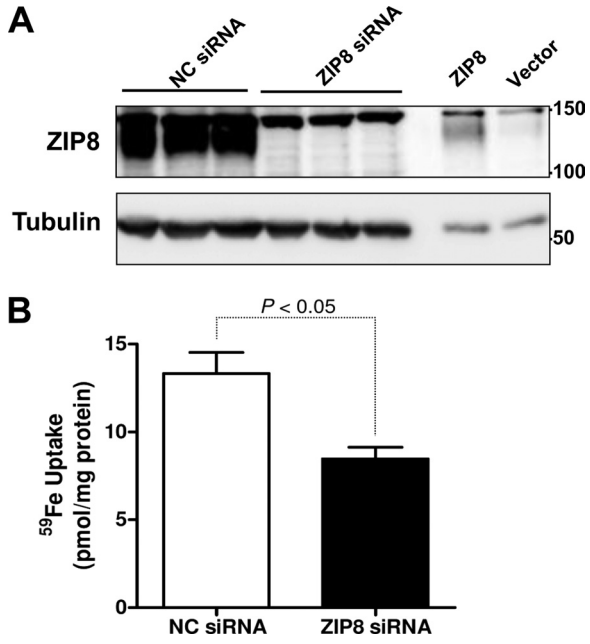

FIGURE 8. **Suppression of ZIP8 expression decreases iron uptake by BeWo cells.** *A*, Western blot analysis of lysates (50 μg of protein) from BeWo cells treated with negative control (*NC*) siRNA or siRNA targeting ZIP8 mRNA. As a positive control for ZIP8, lysates (5 μg of protein) were also analyzed from BeWo cells transfected with pCMV-Sport6 human ZIP8 cDNA (ZIP8) or empty pCMVSport6 vector (*Vector*). *B*, cellular ^{59}Fe uptake in BeWo cells transfected with negative control (*NC*) siRNA or siRNA targeting ZIP8 mRNA. The data represent the means ± S.E. of three independent experiments.

frequently cited as a lysosomal transporter (39, 40), yet in most studies it was detected at the plasma membrane (reviewed in Ref. 16). In a study using Madin-Darby canine kidney cells, ZIP8 abundance at the plasma membrane was found to be responsive to zinc, increasing with zinc depletion and returning to basal levels after zinc repletion (19). Therefore, although we found that zinc increases ZIP8 levels in H4IIE cells, it will be important to determine whether the increase occurs at the plasma membrane. The up-regulation of the zinc/iron importer ZIP8 in response to iron loading may partially account for hepatic zinc accumulation that occurs during iron overload (22, 41–43).

We have previously observed for mouse ZIP14 a pattern of incomplete mutual inhibition and proposed a model in which transport activities of Cd^{2+} and Zn^{2+} differed from the transport activities of other metal ions (9). Whereas 10-fold excess Zn^{2+} entirely abolished $^{55}Fe^{2+}$ uptake, Fe^{2+} only weakly inhibited ZIP14-mediated Zn^{2+} transport (9). In contrast, we found for ZIP8 that 10-fold excess Zn^{2+} did not abolish $^{55}Fe^{2+}$ uptake in oocytes but inhibited $^{55}Fe^{2+}$ uptake by 77% (Fig. 2*B*), *i.e.*, to roughly the extent expected for a 10-fold excess of inhibitor, and we observed mutual inhibition between Fe^{2+} and Zn^{2+} in HEK 293T cells expressing ZIP8 (Fig. 1*C*). Therefore, our observations for ZIP8 — but not ZIP14 — are consistent with a single homogeneous transport pathway (3) shared by Fe^{2+} and Zn^{2+}.

The iron transport activity of ZIP8 along with its partial colocalization with EEA1 raises the possibility that ZIP8 may participate in the cellular assimilation of iron from the transferrin cycle. Specifically, ZIP8 could serve to transport iron from the acidified endosome into the cytosol, a function usually attributed to DMT1 (3) and more recently to ZIP14 (10). However, it should be noted that the iron transport activity of ZIP8 decreases with decreasing pH. At pH 6.5, the pH by which ~50% of the iron dissociates from transferrin-transferrin receptor complex in endosomes (44), ZIP8 showed some iron transport activity in HEK 293T cells but not in oocytes. At pH 5.5, often found in lysosomes, ZIP8 showed no iron transport activity. Thus, it seems unlikely that ZIP8 would function as an iron transporter in lysosomes, where it has been detected (18, 45). Lysosomes play a key role in cellular iron metabolism by degrading the iron storage protein ferritin and releasing the iron into the cytosol, especially during situations such as iron deprivation (46). How iron is transported across the lysosomal membrane remains unknown.

Although the substrate profile of ZIP8 and ZIP14 are similar, they exhibit markedly different tissue expression profiles, suggesting nonredundant functions. In agreement with other studies, we found most abundant ZIP8 expression in the lung (18, 47, 48). The lung is not a significant portal of entry for iron, but other metals such as cadmium and manganese can enter the body in toxic amounts through the lungs (49). It seems clear from our data and others (19) that ZIP8 expressed in oocytes transports cadmium, but in contrast to a previous study (19), we

found that ZIP8 is not an efficient manganese transporter. Indeed our data overall do not support a previous conclusion that ZIP8 acts principally as a manganese transporter under physiologic conditions (19) because (i) manganese transport activity of ZIP8 was very low relative to other metal ions that are more abundant in serum (namely iron and zinc), and (ii) we obtained $K_{0.5}$ for iron of 0.7 μM, substantially lower than that reported for manganese (2.2 μM) (19), suggesting that ZIP8 has a higher affinity for iron than for manganese.

After the lung, the tissue we found that expressed the most ZIP8 was placenta. Strong ZIP8 expression in placenta was also noted in a previous study in which placental ZIP8 expression was second highest out of 16 human tissues after pancreas (and even more abundant than in lung) (18). It is unknown how iron is transported across the placenta to the developing fetus (50). We do know, however, that DMT1 and ZIP14 are not required for maternofetal iron transfer because *Dmt1* and *Zip14* (*Slc39a14*) knock-out mice are born alive with adequate amounts of iron (1, 51). These observations leave ZIP8 as the only remaining known iron transport protein that could function in the placenta, although additional yet to be identified iron transporters may exist.

While our manuscript was under review, Gálvez-Peralta *et al.* (52) reported the characterization of the ZIP8 hypomorphic mouse, which carries a neomycin resistance gene in intron 3 of *Zip8* (*Slc39a8*), resulting in markedly decreased levels of ZIP8 in the embryo, yolk sac, fetus, placenta, and other tissues of neonates. ZIP8 hypomorphic mice exhibit severe anemia as embryos and neonates and do not survive more than 48 h after birth. The anemia appears to result from iron deficiency as indicated by low serum iron, total iron binding capacity, and low hepatic iron. The iron-deficient phenotype of the hypomorphic mice strongly suggests that ZIP8 plays a direct physiologic role in iron metabolism. At the cellular level, ZIP8 seems directly involved, because iron uptake from fetal fibroblasts and liver cells from the hypomorphic mice was found to be significantly impaired. In the ZIP8 hypomorphs, the lower levels of hepatic iron suggest that placental iron transfer is impaired. Consistent with this possibility is our observation that siRNA-mediated knockdown of endogenous ZIP8 reduces iron uptake by BeWo cells, a widely used *in vitro* model system for placental iron transport (28).

The demonstration that ZIP8—and previously ZIP14 (5)—can transport iron raises the question as to whether iron transport activity is a general characteristic of the ZIP family of proteins. In initial screens of the remaining 12 ZIP family members, we have evidence that only one of these, ZIP2, appears capable of transporting iron.[3] Interestingly, previous studies of the *Zip2* knock-out mouse concluded that ZIP2 plays a role in iron homeostasis (53). In an effort to identify which of the 14 ZIP family members might transport iron, we previously examined the effect of iron deficiency and iron overload on the expression of all the ZIP proteins in rat liver (22). We reasoned that iron-regulated ZIP proteins represented the best candidates for possible iron transport activity. However, in that study, ZIP8 mRNA levels did not vary with iron status in rat liver; nor did they vary in H4IIE cells treated with FeNTA. Here we also find that ZIP8 mRNA levels did not vary with iron loading, but ZIP8 protein levels did increase, suggestive of post-transcriptional regulation. These observations highlight the limitation of screening ZIP transporters at the mRNA level.

ZIP proteins generally are predicted to have a long extracellular N-terminal domain, sometimes comprising more than half of the amino acid sequence (54). The N-terminal region, which contains several conserved features including multiple predicted *N*-linked glycosylation sites, has been proposed to modulate metal transport activity (54). The presence of *N*-linked glycosylation has been demonstrated for mouse ZIP4 (55), ZIP5 (56), ZIP8 (19), ZIP14 (57), and human ZIP14 (4) by using the endoglycosidase PNGase F or the glycosylation inhibitor tunicamycin. Here we used PNGase F and tunicamycin to show that rat ZIP8 is glycosylated. Moreover, by using site-directed mutagenesis, we demonstrate that all three predicted *N*-linked glycosylation sites of rat ZIP8 are modified by glycans. Importantly, we found that these *N*-linked glycans are not required for iron or zinc transport by ZIP8 (supplemental Fig. S4). To our knowledge, this is the first direct assessment of the role of glycosylation on metal transport by a ZIP protein.

By using the *Xenopus* oocyte expression system, we found that ZIP8 and ZIP14 efficiently transport cobalt. Indeed, the substrate profiles of ZIP8 and ZIP14 are similar to the ZIP protein ZUPT, which transports zinc, iron, cobalt, and possibly manganese and cadmium in *E. coli* (14). Little is known about mammalian cobalt transport, although some evidence indicates that DMT1 (58, 59) and its homolog Nramp1 (58) can transport cobalt. Intestinal absorption of cobalt has been shown to increase in iron-deficient animals and humans (60, 61), an effect likely mediated through DMT1, which is markedly upregulated in iron-deficient intestine (2). By contrast, it seems unlikely that DMT1 mediates the uptake of cobalt by the liver because hepatic cobalt concentrations are unaffected in mice with hepatocyte-specific deletion of *Dmt1*.[4] Our tissue expression profile data implicate ZIP14 as a likely candidate for hepatic cobalt uptake because liver ZIP14 mRNA levels are ~10 times higher than DMT1 or ZIP8. In the lung, ZIP8 expression is markedly higher than ZIP14 or DMT1, and therefore ZIP8 may represent a major cobalt transporter in this tissue. It is well known that cobalt is absorbed via the lungs (62), which can result in cobalt toxicity, such as in workers occupationally exposed to cobalt-containing dusts. It should be noted, however, that under normal circumstances, the main source of cobalt exposure is food, yet the amount (as inorganic, non-cobalamin cobalt) in typical human diets (<40 μg/day) is markedly lower than the usual amount of iron, zinc, or manganese (2–20 mg/day). In serum, cobalt concentrations (~0.2 ng/ml) are typically less than manganese (~0.6 ng/ml) and at least 3 orders of magnitude lower than those of iron or zinc (~1 μg/ml) (63). Therefore, the principal physiologic substrates of ZIP8 and ZIP14 are likely to be iron and zinc, and to a lesser extent, manganese and cobalt.

[3] W. Zhang and M. Knutson, unpublished observations.

[4] C. Wang and M. Knutson, unpublished observations.

In conclusion, ZIP8 is a novel iron transporter whose expression profile suggests that it may play a role in iron metabolism in the placenta, pancreas, lung, and other organs. The up-regulation of cell-surface ZIP8 by iron loading additionally suggests that ZIP8 may contribute to NTBI uptake during iron overload. Future studies of *Zip8* knock-out animals, especially conditional knock-outs, will be required to define the role(s) of ZIP8 in iron metabolism *in vivo*.

Acknowledgments—We thank Sarah R. Anthony and Colin J. Mitchell (University of Cincinnati) for help in the laboratory.

REFERENCES

1. Gunshin, H., Fujiwara, Y., Custodio, A. O., Direnzo, C., Robine, S., and Andrews, N. C. (2005) Slc11a2 is required for intestinal iron absorption and erythropoiesis but dispensable in placenta and liver. *J. Clin. Invest.* **115,** 1258–1266
2. Gunshin, H., Mackenzie, B., Berger, U. V., Gunshin, Y., Romero, M. F., Boron, W. F., Nussberger, S., Gollan, J. L., and Hediger, M. A. (1997) Cloning and characterization of a mammalian proton-coupled metal-ion transporter. *Nature* **388,** 482–488
3. Fleming, M. D., Romano, M. A., Su, M. A., Garrick, L. M., Garrick, M. D., and Andrews, N. C. (1998) Nramp2 is mutated in the anemic Belgrade (b) rat. Evidence of a role for Nramp2 in endosomal iron transport. *Proc. Natl. Acad. Sci. U.S.A.* **95,** 1148–1153
4. Taylor, K. M., Morgan, H. E., Johnson, A., and Nicholson, R. I. (2005) Structure-function analysis of a novel member of the LIV-1 subfamily of zinc transporters, ZIP14. *FEBS Lett.* **579,** 427–432
5. Liuzzi, J. P., Aydemir, F., Nam, H., Knutson, M. D., and Cousins, R. J. (2006) Zip14 (Slc39a14) mediates non-transferrin-bound iron uptake into cells. *Proc. Natl. Acad. Sci. U.S.A.* **103,** 13612–13617
6. Mackenzie, B., Takanaga, H., Hubert, N., Rolfs, A., and Hediger, M. A. (2007) Functional properties of multiple isoforms of human divalent metal-ion transporter 1 (DMT1). *Biochem. J.* **403,** 59–69
7. Mackenzie, B., Ujwal, M. L., Chang, M. H., Romero, M. F., and Hediger, M. A. (2006) Divalent metal-ion transporter DMT1 mediates both H^+-coupled Fe^{2+} transport and uncoupled fluxes. *Pflugers Arch.* **451,** 544–558
8. Tandy, S., Williams, M., Leggett, A., Lopez-Jimenez, M., Dedes, M., Ramesh, B., Srai, S. K., and Sharp, P. (2000) Nramp2 expression is associated with pH-dependent iron uptake across the apical membrane of human intestinal Caco-2 cells. *J. Biol. Chem.* **275,** 1023–1029
9. Pinilla-Tenas, J. J., Sparkman, B. K., Shawki, A., Illing, A. C., Mitchell, C. J., Zhao, N., Liuzzi, J. P., Cousins, R. J., Knutson, M. D., and Mackenzie, B. (2011) Zip14 is a complex broad-scope metal-ion transporter whose functional properties support roles in the cellular uptake of zinc and nontransferrin-bound iron. *Am. J. Physiol. Cell Physiol.* **301,** C862–C871
10. Zhao, N., Gao, J., Enns, C. A., and Knutson, M. D. (2010) ZRT/IRT-like protein 14 (ZIP14) promotes the cellular assimilation of iron from transferrin. *J. Biol. Chem.* **285,** 32141–32150
11. Eide, D., Broderius, M., Fett, J., and Guerinot, M. L. (1996) A novel iron-regulated metal transporter from plants identified by functional expression in yeast. *Proc. Natl. Acad. Sci. U.S.A.* **93,** 5624–5628
12. Vert, G., Grotz, N., Dédaldéchamp, F., Gaymard, F., Guerinot, M. L., Briat, J. F., and Curie, C. (2002) IRT1, an *Arabidopsis* transporter essential for iron uptake from the soil and for plant growth. *Plant Cell* **14,** 1223–1233
13. Vert, G., Briat, J. F., and Curie, C. (2001) Arabidopsis IRT2 gene encodes a root-periphery iron transporter. *Plant J.* **26,** 181–189
14. Grass, G., Franke, S., Taudte, N., Nies, D. H., Kucharski, L. M., Maguire, M. E., and Rensing, C. (2005) The metal permease ZupT from *Escherichia coli* is a transporter with a broad substrate spectrum. *J. Bacteriol.* **187,** 1604–1611
15. Huynh, C., Sacks, D. L., and Andrews, N. W. (2006) A *Leishmania amazonensis* ZIP family iron transporter is essential for parasite replication within macrophage phagolysosomes. *J. Exp. Med.* **203,** 2363–2375
16. Jenkitkasemwong, S., Wang, C. Y., Mackenzie, B., and Knutson, M. D. (2012) Physiologic implications of metal-ion transport by ZIP14 and ZIP8. *Biometals* **25,** 643–655
17. Eng, B. H., Guerinot, M. L., Eide, D., and Saier, M. H., Jr. (1998) Sequence analyses and phylogenetic characterization of the ZIP family of metal ion transport proteins. *J. Membr. Biol.* **166,** 1–7
18. Begum, N. A., Kobayashi, M., Moriwaki, Y., Matsumoto, M., Toyoshima, K., and Seya, T. (2002) Mycobacterium bovis BCG cell wall and lipopolysaccharide induce a novel gene, BIGM103, encoding a 7-TM protein. Identification of a new protein family having Zn-transporter and Zn-metalloprotease signatures. *Genomics* **80,** 630–645
19. He, L., Girijashanker, K., Dalton, T. P., Reed, J., Li, H., Soleimani, M., and Nebert, D. W. (2006) ZIP8, member of the solute-carrier-39 (SLC39) metal-transporter family. Characterization of transporter properties. *Mol. Pharmacol.* **70,** 171–180
20. Mackenzie, B. (1999) Selected techniques in membrane transport, in *Biomembrane Transport* (Van Winkle, L. J., ed) pp. 327–342, Academic Press, San Diego, CA
21. Gama, L., and Breitwieser, G. E. (2002) Generation of epitope-tagged proteins by inverse polymerase chain reaction mutagenesis. *Methods Mol. Biol.* **182,** 77–83
22. Nam, H., and Knutson, M. D. (2012) Effect of dietary iron deficiency and overload on the expression of ZIP metal-ion transporters in rat liver. *Biometals* **25,** 115–124
23. Chua, A. C., Olynyk, J. K., Leedman, P. J., and Trinder, D. (2004) Nontransferrin-bound iron uptake by hepatocytes is increased in the Hfe knockout mouse model of hereditary hemochromatosis. *Blood* **104,** 1519–1525
24. Morgan, E. H., Smith, G. D., and Peters, T. J. (1986) Uptake and subcellular processing of ^{59}Fe-^{125}I-labelled transferrin by rat liver. *Biochem. J.* **237,** 163–173
25. Besecker, B., Bao, S., Bohacova, B., Papp, A., Sadee, W., and Knoell, D. L. (2008) The human zinc transporter SLC39A8 (Zip8) is critical in zinc-mediated cytoprotection in lung epithelia. *Am. J. Physiol. Lung Cell Mol. Physiol.* **294,** L1127–L1136
26. Lu, J. P., Hayashi, K., and Awai, M. (1989) Transferrin receptor expression in normal, iron-deficient and iron-overloaded rats. *Acta Pathol. Jpn.* **39,** 759–764
27. Bierings, M. B., Baert, M. R., van Eijk, H. G., and van Dijk, J. P. (1991) Transferrin receptor expression and the regulation of placental iron uptake. *Mol. Cell. Biochem.* **100,** 31–38
28. Heaton, S. J., Eady, J. J., Parker, M. L., Gotts, K. L., Dainty, J. R., Fairweather-Tait, S. J., McArdle, H. J., Srai, K. S., and Elliott, R. M. (2008) The use of BeWo cells as an *in vitro* model for placental iron transport. *Am. J. Physiol. Cell Physiol.* **295,** C1445–C1453
29. Taylor, K. M., Morgan, H. E., Johnson, A., Hadley, L. J., and Nicholson, R. I. (2003) Structure-function analysis of LIV-1, the breast cancer-associated protein that belongs to a new subfamily of zinc transporters. *Biochem. J.* **375,** 51–59
30. Grootveld, M., Bell, J. D., Halliwell, B., Aruoma, O. I., Bomford, A., and Sadler, P. J. (1989) Non-transferrin-bound iron in plasma or serum from patients with idiopathic hemochromatosis. Characterization by high performance liquid chromatography and nuclear magnetic resonance spectroscopy. *J. Biol. Chem.* **264,** 4417–4422
31. Craven, C. M., Alexander, J., Eldridge, M., Kushner, J. P., Bernstein, S., and Kaplan, J. (1987) Tissue distribution and clearance kinetics of non-transferrin-bound iron in the hypotransferrinemic mouse. A rodent model for hemochromatosis. *Proc. Natl. Acad. Sci. U.S.A.* **84,** 3457–3461
32. Brissot, P., and Loréal, O. (2002) Role of non-transferrin-bound iron in the pathogenesis of iron overload and toxicity. *Adv. Exp. Med. Biol.* **509,** 45–53
33. Parkes, J. G., Hussain, R. A., Olivieri, N. F., and Templeton, D. M. (1993) Effects of iron loading on uptake, speciation, and chelation of iron in cultured myocardial cells. *J. Lab. Clin. Med.* **122,** 36–47
34. Randell, E. W., Parkes, J. G., Olivieri, N. F., and Templeton, D. M. (1994) Uptake of non-transferrin-bound iron by both reductive and nonreductive processes is modulated by intracellular iron. *J. Biol. Chem.* **269,** 16046–16053
35. Richardson, D. R., Chua, A. C., and Baker, E. (1999) Activation of an iron

uptake mechanism from transferrin in hepatocytes by small-molecular-weight iron complexes. Implications for the pathogenesis of iron-overload disease. *J. Lab. Clin. Med.* **133,** 144–151
36. Scheiber-Mojdehkar, B., Sturm, B., Plank, L., Kryzer, I., and Goldenberg, H. (2003) Influence of parenteral iron preparations on non-transferrin bound iron uptake, the iron regulatory protein and the expression of ferritin and the divalent metal transporter DMT-1 in HepG2 human hepatoma cells. *Biochem. Pharmacol.* **65,** 1973–1978
37. Borgna-Pignatti, C., Rugolotto, S., De Stefano, P., Zhao, H., Cappellini, M. D., Del Vecchio, G. C., Romeo, M. A., Forni, G. L., Gamberini, M. R., Ghilardi, R., Piga, A., and Cnaan, A. (2004) Survival and complications in patients with thalassemia major treated with transfusion and deferoxamine. *Haematologica* **89,** 1187–1193
38. Kumfu, S., Chattipakorn, S., Srichairatanakool, S., Settakorn, J., Fucharoen, S., and Chattipakorn, N. (2011) T-type calcium channel as a portal of iron uptake into cardiomyocytes of β-thalassemic mice. *Eur. J. Haematol.* **86,** 156–166
39. Lichten, L. A., and Cousins, R. J. (2009) Mammalian zinc transporters. Nutritional and physiologic regulation. *Annu. Rev. Nutr.* **29,** 153–176
40. Aydemir, T. B., Liuzzi, J. P., McClellan, S., and Cousins, R. J. (2009) Zinc transporter ZIP8 (SLC39A8) and zinc influence IFN-γ expression in activated human T cells. *J. Leukocyte Biol.* **86,** 337–348
41. Vayenas, D. V., Repanti, M., Vassilopoulos, A., and Papanastasiou, D. A. (1998) Influence of iron overload on manganese, zinc, and copper concentration in rat tissues *in vivo*. Study of liver, spleen, and brain. *Int. J. Clin. Lab. Res.* **28,** 183–186
42. Zhang, Y., Li, B., Chen, C., and Gao, Z. (2009) Hepatic distribution of iron, copper, zinc and cadmium-containing proteins in normal and iron overload mice. *Biometals* **22,** 251–259
43. Adams, P. C., Bradley, C., and Frei, J. V. (1991) Hepatic zinc in hemochromatosis. *Clin. Invest. Med.* **14,** 16–20
44. Núñez, M. T., Gaete, V., Watkins, J. A., and Glass, J. (1990) Mobilization of iron from endocytic vesicles. The effects of acidification and reduction. *J. Biol. Chem.* **265,** 6688–6692
45. Aydemir, T. B., Sitren, H. S., and Cousins, R. J. (2012) The zinc transporter Zip14 influences c-Met phosphorylation and hepatocyte proliferation during liver regeneration in mice. *Gastroenterology* **142,** 1536–1546.e5
46. Kidane, T. Z., Sauble, E., and Linder, M. C. (2006) Release of iron from ferritin requires lysosomal activity. *Am. J. Physiol. Cell Physiol.* **291,** C445–C455
47. Dalton, T. P., He, L., Wang, B., Miller, M. L., Jin, L., Stringer, K. F., Chang, X., Baxter, C. S., and Nebert, D. W. (2005) Identification of mouse SLC39A8 as the transporter responsible for cadmium-induced toxicity in the testis. *Proc. Natl. Acad. Sci. U.S.A.* **102,** 3401–3406
48. Wang, B., Schneider, S. N., Dragin, N., Girijashanker, K., Dalton, T. P., He, L., Miller, M. L., Stringer, K. F., Soleimani, M., Richardson, D. D., and Nebert, D. W. (2007) Enhanced cadmium-induced testicular necrosis and renal proximal tubule damage caused by gene-dose increase in a Slc39a8-transgenic mouse line. *Am. J. Physiol. Cell Physiol.* **292,** C1523–C1535
49. Jarup, L. (2002) Cadmium overload and toxicity. *Nephrol. Dial. Transplant.* **17,** (Suppl. 2) 35–39
50. McArdle, H. J., Lang, C., Hayes, H., and Gambling, L. (2011) Role of the placenta in regulation of fetal iron status. *Nutr. Rev.* **69,** (Suppl. 1) S17–S22
51. Hojyo, S., Fukada, T., Shimoda, S., Ohashi, W., Bin, B. H., Koseki, H., and Hirano, T. (2011) The zinc transporter SLC39A14/ZIP14 controls G-protein coupled receptor-mediated signaling required for systemic growth. *PloS one* **6,** e18059
52. Gálvez-Peralta, M., He, L., Jorge-Nebert, L. F., Wang, B., Miller, M. L., Eppert, B. L., Afton, S., and Nebert, D. W. (2012) ZIP8 zinc transporter. Indispensable role for both multiple-organ organogenesis and hematopoiesis in utero. *PLoS One* **7,** e36055
53. Peters, J. L., Dufner-Beattie, J., Xu, W., Geiser, J., Lahner, B., Salt, D. E., and Andrews, G. K. (2007) Targeting of the mouse Slc39a2 (Zip2) gene reveals highly cell-specific patterns of expression, and unique functions in zinc, iron, and calcium homeostasis. *Genesis* **45,** 339–352
54. Fukada, T., and Kambe, T. (2011) Molecular and genetic features of zinc transporters in physiology and pathogenesis. *Metallomics* **3,** 662–674
55. Wang, F., Kim, B. E., Dufner-Beattie, J., Petris, M. J., Andrews, G., and Eide, D. J. (2004) Acrodermatitis enteropathica mutations affect transport activity, localization and zinc-responsive trafficking of the mouse ZIP4 zinc transporter. *Hum. Mol. Genet.* **13,** 563–571
56. Wang, F., Kim, B. E., Petris, M. J., and Eide, D. J. (2004) The mammalian Zip5 protein is a zinc transporter that localizes to the basolateral surface of polarized cells. *J. Biol. Chem.* **279,** 51433–51441
57. Girijashanker, K., He, L., Soleimani, M., Reed, J. M., Li, H., Liu, Z., Wang, B., Dalton, T. P., and Nebert, D. W. (2008) Slc39a14 gene encodes ZIP14, a metal/bicarbonate symporter. Similarities to the ZIP8 transporter. *Mol. Pharmacol.* **73,** 1413–1423
58. Forbes, J. R., and Gros, P. (2003) Iron, manganese, and cobalt transport by Nramp1 (Slc11a1) and Nramp2 (Slc11a2) expressed at the plasma membrane. *Blood* **102,** 1884–1892
59. Illing, A. C., Shawki, A., Cunningham, C. L., and Mackenzie, B. (2012) Substrate profile and metal-ion selectivity of human divalent metal-ion transporter-1. *J. Biol. Chem.* **287,** 30485–30496
60. Valberg, L. S., Ludwig, J., and Olatunbosun, D. (1969) Alteration in cobalt absorption in patients with disorders of iron metabolism. *Gastroenterology* **56,** 241–251
61. Schade, S. G., Felsher, B. F., Bernier, G. M., and Conrad, M. E. (1970) Interrelationship of cobalt and iron absorption. *J. Lab. Clin. Med.* **75,** 435–441
62. Lauwerys, R., and Lison, D. (1994) Health risks associated with cobalt exposure. An overview. *Sci. Total Environ.* **150,** 1–6
63. Versieck, J. (1985) Trace elements in human body fluids and tissues. *Crit. Rev. Clin. Lab. Sci.* **22,** 97–184